Matrix Effects on Spin−Lattice Relaxation in the Triplet State of Tryptophan

Jie Q. Wu, Andrzej Ozarowski, and August H. Maki*

Department of Chemistry, University of California, Davis, California 95616

Received: April 30, 1997; In Final Form: June 27, 1997[⊗]

Spin−lattice relaxation (SLR) of the photoexcited triplet state of tryptophan both as the free amino acid (Trp) and also incorporated at a buried site of ribonuclease T1 from *Aspergillus oryzae* (RNase T1) is investigated in the ethylene glycol (EG)−water mixed solvent system. Global analysis of microwave-induced delayed phosphorescence (MIDP) transients measured at 1.2 K is employed to obtain the triplet state kinetic parameters over a range of solvent composition between 10 and 90 vol % EG. These parameters are used to calculate the phosphorescence decay profile of the triplet states that contribute to the MIDP. The experimental phosphorescence profile is fitted at each solvent composition as the sum of the calculated nonexponential decay and a simple exponential decay with lifetime equal to the average tryptophan lifetime. The phosphorescence is modeled to originate from two distinct populations characterized by either slow SLR or rapid SLR relative to the triplet state lifetime. Only the former contributes to the MIDP signals while the latter is responsible for the exponential decay component. The fraction of tryptophan undergoing slow SLR, Φ_s, is at a maximum (ca. 0.7) for EG in the range 30−40% (v/v) for both Trp and RNase T1, diminishes sharply with increasing water content, and diminishes slightly with increasing EG content. The SLR of this population is independent of solvent composition. Since the tryptophan triplet state is not kinetically homogeneous in EG−water, the method of microwave-saturated phosphorescence decay analysis produces erroneous kinetic parameters for this system. The native RNase T1 structure becomes unstable above 60 vol % EG as revealed by changes in phosphorescence and ODMR.

Introduction

The phosphorescent triplet state of the amino acid tryptophan has been employed for many years as an "intrinsic" spin probe of the local environment.[1−5] Characteristic shifts of wavelength in the tryptophan phosphorescence spectrum and of zero field splitting (zfs) frequencies that are measured using optical detection of magnetic resonance (ODMR) are associated with such characteristics of the local environment as polarizability, the presence of polar interactions, and aromatic stacking interactions. The bandwidths of the inhomogeneously broadened ODMR transitions measured in zero applied magnetic field may be associated with the heterogeneity of the environment. Tryptophan residues buried in the structured interior of proteins, for instance, exhibit narrower ODMR bandwidths than those exposed to an aqueous solvent environment.

Low-temperature phosphorescence and ODMR measurements typically are made in aqueous buffer that contains a miscible cryosolvent such as ethylene glycol (EG) or glycerin to prevent the formation of ice crystals that could lead to disruption of biopolymer structure and aggregation of solutes. In an attempt to achieve solvent conditions that approach those of natural conditions in a cell, these biomolecules have been frozen into matrixes that contain as little cryosolvent as possible. It has been noticed in the past that although the intensity of the phosphorescence does not vary much as the cryosolvent concentration approaches zero, the intensity of the ODMR signals become vanishingly small as this limit is approached.[6] We have found, in fact, that if EG is reduced below ca. 10% (v/v), the ODMR signals of tryptophan become very weak and exceedingly difficult to detect even at 1.2 K. This is the case for the free amino acid, as well as for tryptophan associated in proteins, even at interior buried sites. This effect also has been observed in the tetraol, 7,8,9,10-tetrahydrotetrahydroxybenzo-[*a*]pyrene, which carries a pyrenyl chromophore, when dissolved in EG−aqueous buffer solvent mixtures.[7] The nature of the phenomena leading to ODMR signal reduction as the water content of the cryosolvent increases has not been completely resolved, however.

Previous ODMR measurements[6] carried out on ribonuclease T1 from *Aspergillus oryzae* (RNase T1) which contains a single buried tryptophan residue suggested that the loss of signal was caused by the enhancement of spin−lattice relaxation (SLR) rates with increasing water content of the glycerol-containing cryosolvent. Enhanced SLR results in reduced spin alignment in the triplet state; the ODMR signal intensities are reduced accordingly. An alternative mechanism, the loss of spin alignment due to solute aggregation resulting in triplet−triplet energy transfer between translationally inequivalent Trp residues, is unlikely. The buried tryptophan residue of the RNase T1 molecule would lie beyond triplet−triplet energy transfer range even if protein aggregation were to occur.

The method used previously[6] to measure SLR rate constants in RNase T1 involves analysis of the phosphorescence decay kinetics during pairwise microwave saturation of the triplet state sublevels.[8] Analysis of the decay curves of the resulting pseudo-two-level system allows one, in principle, to obtain independently the values for the SLR rate constants and the decay constant of each sublevel to the ground singlet state. This method does not always give reliable results, however, as we have demonstrated recently.[9] The major problems arise from (a) the difficulty in completely saturating sublevel populations during the decay, (b) interference from impurity phosphorescence, (c) the requirement that the emission originate from a single population having a unique set of rate constants, i.e., a kinetically homogeneous population, and (d) the fact that there is no redundancy of data; the number of experimentally determined quantities (six) is the same as the number of

* To whom correspondence should be addressed.

[⊗] Abstract published in *Advance ACS Abstracts,* August 15, 1997.

S1089-5639(97)01455-2 CCC: $14.00

independent parameters to be determined, three decay rate constants and three SLR rate constants.

We have developed a method recently for global analysis of sets of microwave-induced delayed phosphorescence (MIDP)[10] responses by computer that allows one to obtain reliably the decay and SLR rate constants of a photoexcited triplet state.[9] Instead of the limited use of only the amplitudes of the MIDP responses that has been customary in the past, the global analysis method seeks to fit by least-squares methods all experimental points of a data set consisting of two or of all three zero field ODMR transitions. For a digitally collected set of MIDP measurements, the total number of fitted data points can approach or exceed 20 000. We have found[9] that if more than one zero field transition is measured and utilized in the global analysis, it is impossible to obtain a satisfactory fitting of the data without including SLR in the kinetic analysis. The complete analysis that incorporates SLR subsequently yields reliable values for all kinetic parameters.

Having available this global analysis method for obtaining SLR rate constants,[9] we report here on its use to investigate the dependence in ethylene glycol (EG)−water mixtures of the kinetic parameters of tryptophan on solvent composition. Both the free amino acid (Trp) and tryptophan incorporated at a buried site in the enzyme RNase T1 were investigated at $T = 1.2$ K. The results of this work are quite surprising. We had anticipated finding a continuous variation of the SLR rate constants of tryptophan with composition of the solvent and that they should increase with increasing water content. What is found, instead, in these solvent mixtures are two major tryptophan populations that differ radically in their SLR properties. One major population undergoes slow SLR at 1.2 K; its triplet state maintains spin alignment during optical pumping and during decay of the triplet state. The SLR rate constants of this population are effectively insensitive to solvent composition over the range investigated (10−90 vol % EG). The phosphorescence of this population decays nonexponentially as expected for a triplet state that maintains spin alignment. The other major population is characterized by rapid SLR at 1.2 K relative to the triplet state lifetime and the absence of spin alignment during phosphorescence decay. The phosphorescence of this population decays exponentially with a decay constant equal to the average of the individual sublevel decay constants. The MIDP measurement (and slow passage ODMR) senses only the first of these populations. The loss of these signals with increasing water content of the solvent is the result of a decrease in the population of the slowly relaxing tryptophan.

We believe that the frozen EG−water solvent contains two major types of local environment, whose populations vary with water content, and that differ radically in their SLR efficiency. In one of these environments energy transfer between the triplet spin states and the lattice phonons is efficient, while for the other type of local environment energy transfer is inefficient. Only the latter population, which decreases sharply with increasing water content in water-rich solvents, contributes to ODMR signals of tryptophan at 1.2 K.

Experimental Part

L-Tryptophan (Trp) (>99.5%) was purchased from Fluka, while RNase T1 from *Aspergillus oryzae* (lyophilized powder) was a product of Sigma. Both were used as received. Ethylene glycol (puriss., ≥99.5%) was obtained from Fluka. It was checked and found to contribute negligible background to the phosphorescence. The solvent consisted of various ratios of EG and 10 mM pH 7 phosphate buffer. The Trp concentration was about 1 mM, while RNase had a concentration of 0.2 mM. Samples were contained in 1 mm i.d. Suprasil tubes that were placed in a copper wire helix terminating a stainless steel coaxial transmission line that was immersed into a liquid He Dewar that could be maintained at 1.2 K by pumping.

The sample was cooled by sudden immersion into liquid nitrogen whenever possible, to encourage the formation of a clear glass. It was then transferred rapidly into the liquid He Dewar containing 1 atm of He gas at 77 K. In the case of the samples having the least EG (10 and 15 vol %) the sample tube generally shattered after immersion into liquid nitrogen, and the sample formed a snow. These samples were cooled more slowly by introducing them into the He gas at 77 K. These slowly cooled samples also formed a snow, indicating the separation of ice crystals. Samples in aqueous 20 vol % EG could be chilled rapidly without shattering, but they also formed a snow. Clear glasses were formed only in solutions containing 30 vol % or more EG. Phosphorescence measurements were made with the sample immersed in He gas at 77 K, as well as after addition of liquid He. For ODMR measurements, the temperature was reduced to 1.2 K by pumping on the liquid He.

Details of the experimental arrangement and methods for ODMR and MIDP measurements have been described previously.[9,11] Samples were excited using the emission of a 100 W Hg arc lamp passsed through a 0.1 m monochromator set at 297 nm using 16 nm band-pass. The phosphorescence was monitored at the peak of the tryptophan 0,0 band using a monochromator bandwidth of 3.2 nm. The incident microwave power (150 mW) and sweep rate (15 GHz/s) were kept constant in the MIDP measurements, and the same portion of the helix was monitored from sample to sample.

Global analysis of the MIDP data sets to obtain sublevel decay constants, k_i, and SLR rate constants, W_{ij} ($i, j = x, y, z$), has been presented earlier.[9] Briefly, using the Simplex algorithm,[12] all of the MIDP data sets are fitted simultaneously by computer to predicted responses based on the decay equations

$$d\mathbf{n}/dt = \mathbf{R}\cdot\mathbf{n} \tag{1}$$

where $\mathbf{n}$ is the vector of sublevel populations, and $\mathbf{R}$ is the rate constant matrix with diagonal elements $-k_i$ (the decay rate constants) and off-diagonal elements W_{ij} (the SLR rate constants). The parameters fitted are the k_i, W_{ij}, $r_{ji} = k_j^{(r)}/k_i^{(r)}$, $n_{ji}^0 = n_j^0/n_i^0$, and F_0, where the $k_i^{(r)}$ are radiative rate constants, the n_i^0 are initial populations when optical pumping is terminated, and F_0, the population transfer factor, is a measure of the transfer achieved by the microwave fast passage. For saturation, $F_0 = 1$, while for population inversion, $F_0 = 2$. The number of independent parameters may be reduced, if necessary to avoid local minima, by introducing constraints, such as the average decay constant, $\langle k\rangle = (1/3)\Sigma\, k_i$, from microwave-saturated decay at 1.2 K[8] or decay under rapid SLR achieved at 4.2 or 77 K, and the relative quantum yield, $Q_j/Q_i = r_{ji}(k_i/k_j)$, from an experiment devised by Shain and Sharnoff.[13]

Phosphorescence Decay Kinetics. In the present work, we go a step farther, using the parameters obtained in the global MIDP analysis to predict the phosphorescence decay kinetics and to compare them with measurements. Having determined the elements of $\mathbf{R}$, we obtain its eigenvalues, ρ_n ($n = 1, 2, 3$), and normalized eigenvectors, $\mathbf{c}_n$ ($\Sigma_n c_{jn} = 1$). Each sublevel population decays according to[14]

$$n_j(t) = n_j^0 \sum_n c_{jn} \exp(\rho_n t) \tag{2}$$

and the phosphorescence decay is given by

$$I(t) = \sum_j n_j(t) k_j^{(r)} \tag{3}$$

TABLE 1: Summary of Characteristic Zero-Field Splitting Parameters[a]

	$D-E$		$2E$		$D+E$			
sample	ν_0 (GHz)	$\nu_{1/2}$ (MHz)[b]	ν_0 (GHz)	$\nu_{1/2}$ (MHz)[b]	ν_0 (GHz)	$\nu_{1/2}$ (MHz)[b]	D (GHz)	E (GHz)
Trp								
10% EG	1.772(1)	65(3)	2.504(4)	131(7)	4.264(−)[c]	84(−)[c]	3.018	1.249
15% EG	1.748(3)	62(6)	2.468(3)	114(2)	4.225(4)	80(2)	2.987	1.237
20% EG	1.758(2)	56(1)	2.515(6)	129(5)	4.253(4)	82(7)	3.005	1.252
30% EG	1.779(5)	69(1)	2.490(2)	123(6)	4.262(2)	83(4)	3.020	1.243
40% EG	1.766(3)	50(2)	2.513(7)	103(1)	4.277(2)	74(2)	3.021	1.256
50% EG	1.764(3)	58(1)	2.515(3)	143(5)	4.246(6)	81(4)	3.005	1.249
60% EG	1.762(2)	53(1)	2.485(5)	117(1)	4.250(3)	84(4)	3.006	1.243
90% EG	1.770(2)	65(2)	2.363(2)	169(7)	4.226(3)	84(1)	2.998	1.205
RNase T_1								
15% EG	1.758(4)	42(5)	2.457(2)	54(2)	4.223(12)	36(3)	2.991	1.231
20% EG	1.750(3)	34(2)	2.471(4)	51(3)	4.240(−)[c]	56(−)[c]	2.995	1.238
30% EG	1.765(2)	34(7)	2.505(2)	75(5)	4.223(9)	26(9)	2.994	1.241
40% EG	1.751(3)	35(2)	2.476(3)	54(1)	4.243(3)	33(6)	2.997	1.242
50% EG	1.756(2)	33(1)	2.473(3)	50(2)	4.237(−)[c]	54(−)[c]	2.996	1.239
60% EG	1.755(3)	40(2)	2.466(4)	55(2)	4.239(−)[c]	30(−)[c]	2.997	1.238
90% EG	1.701(2)	51(2)	2.522(8)	122(11)	4.212(−)[c]	74(−)[c]	2.956	1.258

[a] The standard deviation (σ) in last digit given in parentheses. Measurements were made at 1.2 K. [b] $\nu_{1/2}$ is half-width at half-maximum intensity. [c] σ not reported; only two measurements were averaged.

In terms of the parameters obtained from the global MIDP analysis, the phosphorescence kinetics can be expressed as

$$I(t) = \sum_{j,n} c_{jn} r_{ji} n_{ji}^{\ 0} \exp(\rho_n t) \qquad (4)$$

Relation of Initial Phosphorescence Intensities to Populations. We will be interested in converting the initial phosphorescence intensities, $I(0)$, of triplet states undergoing fast or slow SLR (which we obtain from fitting the phosphorescence decay kinetics, see below) to their initial populations, n_f^0 or n_s^0, respectively. The population ratio differs from the intensity ratio since the sublevel occupancies are essentially equal in the former population, but spin alignment is present in the latter.

It may be verified readily that

$$n_s^{\ 0}/n_f^{\ 0} = [(\sum_j r_{ji})(\sum_j n_{ji}^{\ 0})/3(\sum_j r_{ji}\, n_{ji}^{\ 0})][I_s(0)/I_f(0)] \qquad (5)$$

Then, the fraction of the population exhibiting slow SLR is

$$\Phi_s = (n_s^{\ 0}/n_f^{\ 0})/[1 + (n_s^{\ 0}/n_f^{\ 0})] \qquad (6)$$

Effective Population Transfer Factor, F. F_0 is the transfer factor that refers to the population that responds in the MIDP experiment. If only a fraction of the population is involved, the analysis[9] produces an effective transfer factor, F. Since F is obtained through normalization by the initial phosphorescence intensity $I(0) = I_s(0) + I_f(0)$, it is related to F_0 by

$$F = F_0[I_s(0)/I(0)] \qquad (7)$$

Results

The phosphorescence spectra of Trp and of RNase T1 in aqueous EG have been reported previously.[2,15] The spectrum of RNase T1 is particularly well-resolved at liquid He temperatures, characteristic of a Trp residue buried in a very homogeneous protein environment.[2]

Delayed slow-passage ODMR measurements[15] were carried out on all three zero field ODMR transitions in order to obtain the ODMR frequencies, line widths, and zfs parameters. These data are listed in Table 1. The data reveal no particular trend in the ODMR frequencies or line widths as the solvent composition is varied up to an EG content of 60 vol %. Minor fluctuations in the measured values are seen, however, that are outside of the standard deviation of the individual data sets[15] and could represent the effect of differences in sample histories. Significant changes in the properties of Trp and of RNase T1 at higher EG content (90 vol %) are observed, which will be discussed below.

The triplet state kinetic parameters obtained from global analysis of the MIDP data sets are listed in Table 2. The SLR rate constants, W_{ij}, reveal fluctuations that are outside of the estimated standard error,[9] but there is no trend with solvent composition. Specifically, SLR does not increase with an increase in the water content of the sample for either Trp or RNase T1. The k_i are independent of solvent composition within experimental error. The triplet lifetime obtained from least-squares fitting of the simple exponential decay of all samples at 4.2 or 77 K (rapid SLR conditions) is 6.6 ± 0.1 s for RNase T1 and 7.1 ± 0.1 s for Trp. No effect of solvent composition on the sublevel decay constants is detectable.

Figure 1 shows the phosphorescence decay kinetics of Trp in 20% (v/v) EG/water at 1.2 K. The decay clearly is nonexponential, in contrast with the simple exponential decay exhibited at 4.2 K (not shown), indicating that the sublevels have become decoupled as a result of quenching SLR. Also shown in Figure 1 (dashed curve) is the predicted phosphorescence decay from eq 4 based on the analysis outlined in the previous section using the experimental parameters from Table 2. The experimental decay clearly deviates from that expected from the MIDP analysis; it appears to approach a simple exponential decay more closely. Assuming that a subpopulation is present in the sample that is responsible for the kinetic behavior obtained from global analysis of MIDP, we scaled down the calculated contribution of this population to $I(0)$. Figure 2 shows the result of scaling the contribution of the population giving rise to the MIDP signals to 42% of $I(0)$. This scaled decay in Figure 2 is labeled *b*. When the scaled decay is subtracted from the experimental decay (Figure 2, curve a), the residual contribution to the phosphorescence decay is found to be a simple exponential (Figure 2, curve c). Furthermore, the lifetime of this component (58% of $I(0)$) is found to be 7.0 s, exactly the same as the Trp phosphorescence lifetime in 20% EG/water measured under rapid SLR conditions at 4.2 K.

The poor agreement between the decay expected from the MIDP analysis and the measured decay that is characterized in Figure 1 also was found for samples of RNase T1. Figure 3 shows the phosphorescence decay of RNase T1 in 15% (v/v) EG/buffer (curve a) and the predicted decay curve from MIDP scaled down to 28% of $I(0)$ (curve b). The difference curve,

TABLE 2: Summary of Characteristic Kinetic Parameters[a]

sample	k_x (s^{-1})[b]	k_y (s^{-1})[b]	k_z (s^{-1})[b]	W_{xy} (s^{-1})	W_{xz} (s^{-1})	W_{yz} (s^{-1})	r_{yx}[c]	n_{yx}^0	n_{zx}^0	$\bar{\tau}$ (s)[d]
Trp										
10% EG	0.35(1)	0.078(9)	0.000(2)	0.09(1)	0.07(1)	0.041(4)	0.00(1)	1.43(5)	1.40(5)	7.0
15% EG	0.34(1)	0.082(6)	0.000(4)	0.03(5)	0.025(6)	0.062(1)	0.044(8)	1.79(2)	1.36(1)	7.1
20% EG	0.32(4)	0.11(2)	0.000(8)	0.05(1)	0.04(2)	0.054(2)	0.01(3)	1.51(7)	1.49(7)	7.0
30% EG	0.32(1)	0.094(5)	0.008(4)	0.000(4)	0.022(5)	0.034(1)	0.11(1)	2.58(7)	1.49(2)	7.1
40% EG	0.31(1)	0.107(7)	0.003(4)	0.016(4)	0.017(6)	0.052(1)	0.09(1)	1.83(3)	1.44(2)	7.1
50% EG	0.31(1)	0.102(5)	0.000(3)	0.013(4)	0.041(5)	0.042(1)	0.120(8)	1.71(3)	1.40(2)	7.3
60% EG	0.32(3)	0.10(1)	0.01(1)	0.01(1)	0.02(1)	0.051(2)	0.12(3)	1.75(6)	1.35(3)	7.0
90% EG	0.32(2)	0.11(1)	0.000(5)	0.021(7)	0.03(2)	0.058(1)	0.11(2)	2.00(8)	1.47(4)	7.0
RNase T_1										
15% EG	0.37(5)	0.08(1)	0.010(6)	0.05(2)	0.10(2)	0.02(1)	0.01(2)	1.8(2)	1.25(6)	6.5
20% EG	0.34(7)	0.08(2)	0.04(1)	0.01(3)	0.07(3)	0.02(1)	0.17(3)	1.6(2)	1.6(2)	6.5
30% EG	0.33(9)	0.12(4)	0.01(2)	0.02(3)	0.03(4)	0.136(5)	0.14(6)	1.6(2)	1.4(1)	6.5
40% EG	0.32(7)	0.09(4)	0.05(3)	0.00(3)	0.01(4)	0.063(6)	0.18(6)	1.6(2)	1.4(1)	6.5
50% EG	0.32(14)	0.10(6)	0.02(4)	0.01(5)	0.03(7)	0.088(4)	0.14(9)	1.6(4)	1.4(3)	6.8
60% EG	0.322(8)	0.116(4)	0.018(3)	0.020(4)	0.023(3)	0.21(2)	0.178(7)	1.75(2)	1.22(4)	6.6

[a] The standard error (σ_e) in last digit is given in parentheses. Measurements were made at 1.2 K unless otherwise noted. [b] $1/\bar{\tau} = (k_x + k_y + k_z)/3$ fixed in the analysis. [c] $r_{zx} = 0$ for all samples within experimental error. [d] Single-exponential decay lifetime. Measured at 4.2 or 77 K, where sublevel population undergoes rapid SLR.

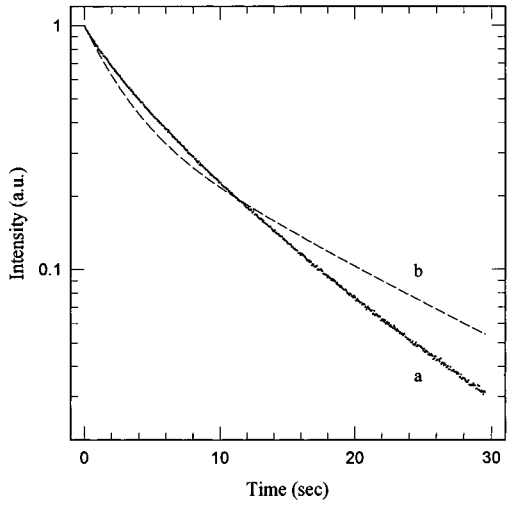

Figure 1. Normalized phosphorescence decay of Trp in 20% (v/v) EG/water at 1.2 K: (a) experimental decay; (b) predicted decay from eq 4 based on the parameters from MIDP analysis given in Table 2, assuming that emission originates totally from triplet states responsible for the MIDP signals.

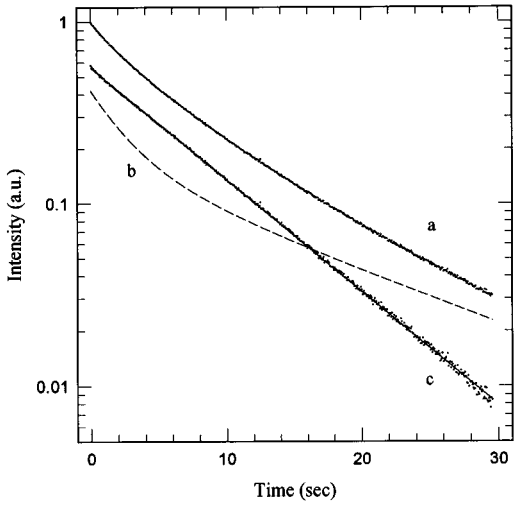

Figure 2. Deconvolution of the phosphorescence decay of Trp in 20% (v/v) EG/water at 1.2 K: (a) normalized experimental decay as in Figure 1; (b) component giving rise to the MIDP signals scaled to 42% of $I(0)$; (c) the residual decay component (curve a minus curve b). The superimposed solid line is a least-squares single-exponential fitting of the residual yielding $\tau = 7.0$ s.

representing 72% of $I(0)$ and shown as curve c, is a simple exponential with a lifetime of 6.9 s, which is close to that measured for RNase T1 under rapid SLR conditions (Table 2).

As the EG content of the solvent is increased, treatments such as those described above yield simple exponential decays as residuals with lifetimes close to those exhibited by the sample under rapid SLR conditions. However, the calculated nonexponentially decaying portion comprises an increasingly larger fraction of $I(0)$. The contribution of this component appears to reach a maximum for EG/water mixtures in the 30−40% range. The analysis for Trp in 40% EG/water appears in Figure 4. In this case the nonexponential component has increased to 60% of $I(0)$; the lifetime of the exponential component is 8.0 s, close to the 7.1 s lifetime measured at 4.2 K (Table 2). For Trp in 50%, 60%, and 90% EG/water solvent, the contribution of nonexponential decay decreases somewhat to ca. 50% of $I(0)$.

Similar behavior with respect to solvent composition is exhibited by RNase T1. The analysis of its phosphorescence decay in 40% EG/buffer is shown in Figure 5. The deconvolution yields a nonexponential component based on global MIDP analysis that is 62% of $I(0)$. The exponential component has a lifetime of 8.2 s, which is somewhat longer than the 6.5 s lifetime of this sample at 4.2 K (Table 2), but probably within the range of error to be expected for the deconvolution procedure. The decay of RNase T1 in 50% and 60% EG/buffer reveals an additional complexity, as shown in Figure 6 for the 60% EG/buffer sample. The closest approach to a simple exponential residual decay was found by scaling the calculated nonexponential part (from MIDP) to 55% of $I(0)$. The residual (curve c) is largely exponential ($\tau = 6.3$ s), but a minor initial rapid decay component also is present. A similar rapid decay component also is found, but with even less amplitude, in the residual obtained for RNase T1 in 50% EG/buffer ($\tau = 6.7$ s, analysis not shown). When the EG content of the solvent is increased to 90 vol %, the rapid component that accompanies the residual is found to have increased considerably. The phosphorescence spectra of RNase T1 in 15%, 60%, and 90% EG at 77 K are compared in Figure 7. The increase in the intensity of a blue-shifted component that we attribute to tyrosine phosphorescence is apparent with increasing EG. Slow passage ODMR measurements, monitoring the blue-shifted emission in 90% EG, reveal a response at 5.59 GHz that is characteristic of the tyrosine triplet state.[3,16] These spectral changes indicate that as the EG content of the solvent increases above ca. 60 vol %, the native structure of RNase T1 becomes increasingly unstable. As the compact structure of the enzyme unravels, the tryptophan residue moves away from the neighborhood of the tyrosines (which it quenches by singlet−singlet energy transfer in the

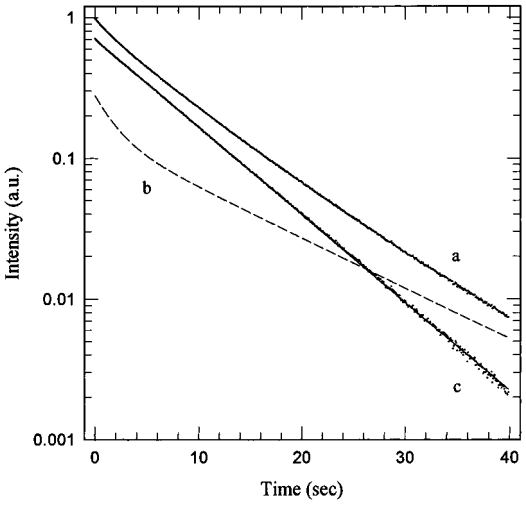

Figure 3. Deconvolution of the phosphorescence decay of RNase T1 in 15% (v/v) EG/water at 1.2 K: (a) normalized experimental decay; (b) component giving rise to the MIDP signals calculated from data in Table 2 using eq 4 and scaled to 28% of $I(0)$; (c) the residual decay component (curve a minus curve b). The superimposed solid line is a least-squares single-exponential fitting of the residual yielding $\tau = 6.9$ s.

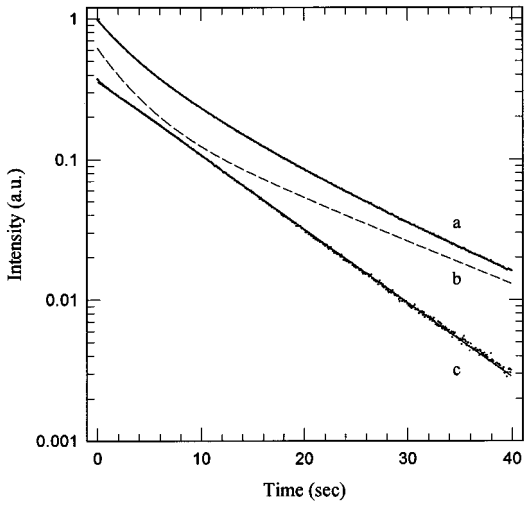

Figure 5. Deconvolution of the phosphorescence decay of RNase T1 in 40% (v/v) EG/water at 1.2 K: (a) normalized experimental decay; (b) calculated component giving rise to the MIDP signals using eq 4 with data from Table 2 with scaling to 62% of $I(0)$; (c) the residual component (curve a minus curve b). The superimposed solid line is a least-squares single-exponential fitting of the residual giving $\tau = 8.2$ s.

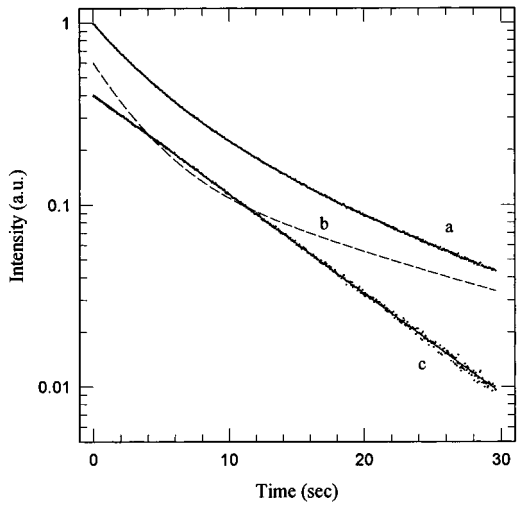

Figure 4. Deconvolution of the phosphorescence decay of Trp in 40% (v/v) EG/water at 1.2 K: (a) normalized experimental decay; (b) calculated component giving rise to the MIDP signals using eq 4 with data from Table 2 and scaled to 60% of $I(0)$; (c) the residual component (curve a minus curve b). The superimposed solid line is a least-squares single-exponential fitting of the residual giving $\tau = 8.0$ s.

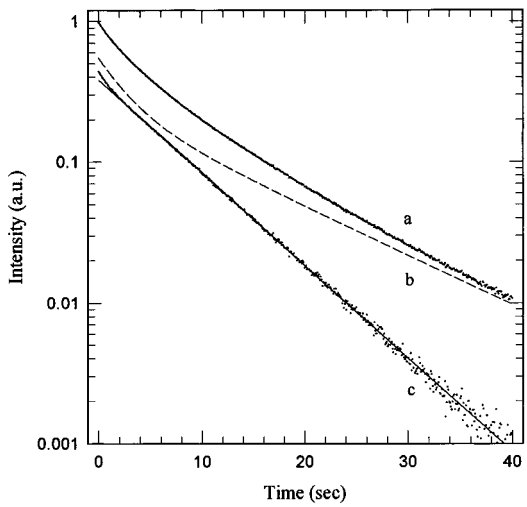

Figure 6. Deconvolution of phosphorescence decay of RNase T1 in 60% (v/v) EG/water at 1.2 K: (a) normalized experimental decay; (b) calculated component giving rise to the MIDP signals using eq 4 with data from Table 2 with scaling to 55% of $I(0)$; (c) the residual component (curve a minus curve b). The superimposed solid line is a least-squares single-exponential fitting that yields $\tau = 6.3$ s. The short-lived initial deviation of the residual from a single exponential is assigned to tyrosine phosphorescence.

native structure); the tyrosines then become luminescent. This solvent-induced denaturation is confirmed by the spectral changes in the tryptophan phosphorescence that are observed when the EG content is increased to 90%. The 0,0 band peak wavelength increases from 406.0 nm in 15% EG to 409.8 nm in 90% EG, and the resolution of the spectrum is reduced, indicating an increase in heterogeneity of the tryptophan environment. The zfs parameters of RNase T1 obtained in 90% EG (Table 1) differ considerably from those found at the lower EG concentrations, where the native structure is dominant and the ODMR bandwidths also are greater, having become comparable to those of Trp. The zfs parameters differ by a great deal from those of Trp in 90% EG, however, indicating that the protein still is involved in the local interactions. The rapidly decaying component of the RNase T1 phosphorescence that grows in with increasing EG content of the solvent originates from tyrosine, which has a considerably shorter triplet lifetime than tryptophan.[3] Deviation of the residual from simple exponential behavior was not observed in any of the Trp samples.

Aside from the interference from tyrosine, we found that we could fit the phosphorescence decay of each sample to the sum of a simple exponential decay and a nonexponential decay that was predicted from the global analysis of MIDP data. Furthermore, the lifetime of the simple exponential decay was found to be close to that of the tryptophan triplet state under rapid SLR conditions.

Using eqs 5 and 6, we have calculated Φ_s, the fraction of the triplet population that decays with slow SLR (revealed by the global MIDP analysis), vs solvent composition. The results are plotted in Figure 8. The similar behavior of Trp and RNase T1 as the composition of the solvent is varied is noteworthy.

The effective saturation factor, F, that arises from the global analysis of MIDP is equal to the actual degree of saturation of

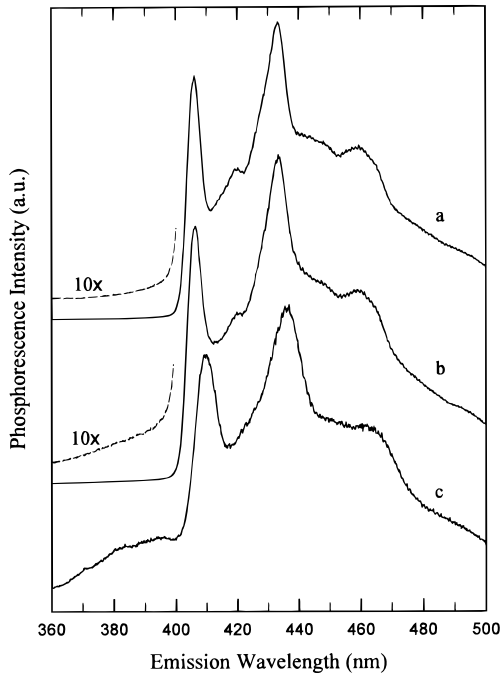

Figure 7. Normalized phosphorescence spectra of RNase T1 in (a) 15%, (b) 60%, and (c) 90% EG/water (v/v) at 77 K. The broad emission to the blue of 400 nm is assigned to tyrosine.

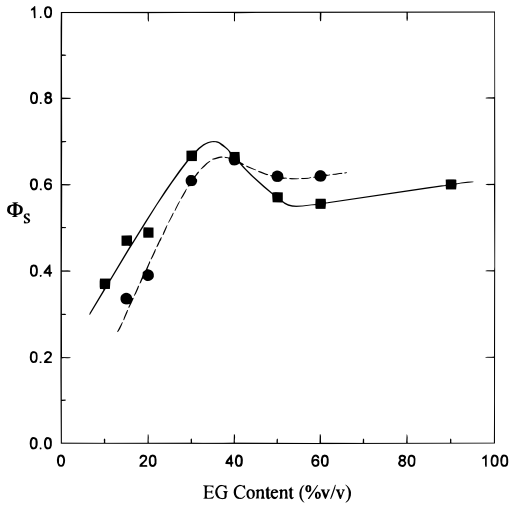

Figure 8. Influence of solvent composition on the fraction of the triplet population that is characterized by slow SLR and is responsible for the observed MIDP signals, calculated using eqs 5 and 6. Trp data are plotted as squares and the RNase T1 data as circles. The RNase T1 data point for 60% EG has been corrected for the tyrosine phosphorescence component (Figure 6). The smooth curves are only to guide the eye.

the sublevel populations by the microwave fast passage, F_0, only if the entire triplet population is kinetically homogeneous. Our interpretation of the present data is that only a fraction of the triplet population produces a MIDP response, the remainder being characterized by rapid SLR and the absence of spin alignment. Thus, to the extent that experimental conditions of the MIDP measurements are held constant from sample to sample, eq 7 should hold and F should plot linearly against $I_s(0)/I(0)$ with a slope of F_0. Plots of F vs $I_s(0)/I(0)$ for both Trp and RNase T1 that exhibit the expected relationship (eq 7) are shown in Figure 9. For Trp, we find that $F_0 = 1.34$, indicating that, under the experimental conditions employed, the sublevel populations of the slowly relaxing triplet states are partially inverted by the microwave fast passage. On the other hand, $F_0 = 1.05$ for RNase T1, indicating that the sublevel populations are just saturated under the same conditions. A

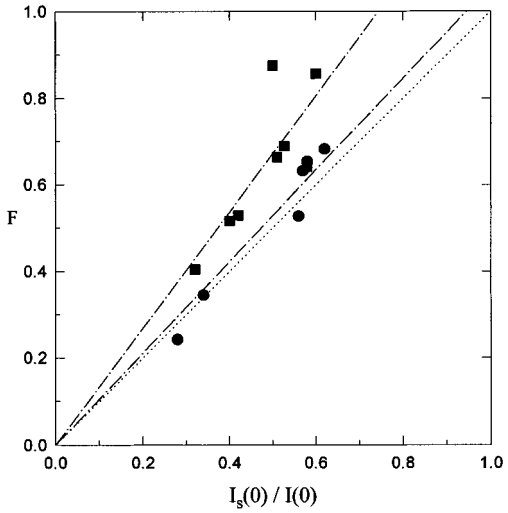

Figure 9. Dependence of the effective saturation factor, F, on the fraction of $I(0)$ that originates from triplet states with slow SLR and give rise to the MIDP signals. Trp data are plotted as squares and the RNase T1 data as circles. The dotted line represents $F_0 = 1$. The dot-dashed lines are least-squares fittings yielding $F_0 = 1.34$ and 1.05 for Trp and RNase T1, respectively.

smaller F_0 for RNase T1 could be the result of narrower intrinsic ODMR line widths and, thus, a fast passage traversal time that is insufficient to produce inversion of the sublevel populations.

Discussion

In this report, we have employed a method of global analysis of MIDP responses[9] to determine the triplet state sublevel kinetic and radiative parameters of Trp and RNase T1 in low-temperature aqueous EG solvents. The overall phosphorescence decay kinetics of the samples were compared with those predicted from global MIDP analysis. The experimental kinetics deviate from those predicted. The predicted decay curve, with reduced intensity, when subtracted from the experimental decay curve produces a residual that displays simple exponential kinetics with decay constant equal to that exhibited by the sample under rapid SLR conditions (Figures 2−6). These results are interpreted on the basis of two distinct populations of phosphorescent triplet states: (a) a population with slow SLR, i.e., decoupled sublevel populations, that is responsible for the MIDP responses and (b) a population undergoing rapid SLR, i.e., coupled sublevel populations, that does not contribute to the MIDP responses but is responsible for the exponentially decaying residual. The relative amounts of the decoupled and coupled populations depend on the overall composition of the solvent. This interpretation is supported by the observation that F, the effective population transferred in the microwave rapid passage, varies linearly with $I_s(0)/I(0)$, the fraction of phosphorescence emitted by the decoupled triplet states (Figure 9).

The model that we have adopted consisting of two populations with discrete SLR behavior is the simplest possible that is consistent with the MIDP and phosphorescence kinetics. It is likely that a continuous distribution of SLR rate constants could be proposed that also would satisfy the kinetic behavior. A distribution of SLR rate constants that peaks near the values obtained from analysis of the MIDP data and falls off sharply at higher values probably could be found that fits the data equally well.

Although the ODMR and MIDP measurements do not yield information on the coupled triplet population, we find that the zfs, ODMR line widths, and SLR parameters of the decoupled population are insensitive to the overall composition of the solvent up to 60% EG, suggesting that the local solvent structure

of this population does not vary very much from sample to sample. What does vary, however, is the fraction of triplet states that have this local solvent structure. As the EG content is reduced below ca. 30% (v/v), the fraction of decoupled triplet states decreases sharply, and the ODMR and MIDP signals become increasingly difficult to detect. The fraction of decoupled tryptophan triplet states appears to reach a maximum at a solvent composition of 30−40 vol % EG for both Trp and RNase T1, dropping somewhat at higher EG content. The maximum fraction of decoupled triplet states is approximately 0.7.

As the EG is increased above ca. 60 vol %, the native structure of RNase T1 becomes unstable. The resulting protein is characterized by tyrosine emission (quenched in the native structure) and tryptophan triplet state properties that reflect a more heterogeneous local environment than is found in the native state (Figure 7; Table 1, 90% EG). These changes are consistent with denaturation of RNase T1 to a more random structure. The zfs of Trp also are changed significantly, and the ODMR bandwidths are increased in 90% EG, reflecting significant changes in the local environment of the decoupled triplet states.

The physical state of the sample is an important consideration in evaluating the results of these measurements. The water−EG liquid/solid phase diagram has been reported recently.[17] It is characterized by a 1:1 hydrate corresponding to 77.5 mass % EG, which melts at ca. − 42 °C and is spanned by two eutectic points. The system has a strong tendency to supercool to form a glass, particularly in the composition range between 55 and 85 mass % EG. Rapid cooling of our samples containing 30 vol % or more EG produced a clear glass with no evidence of phase separation. On the other hand, the samples containing 10−20 vol % EG became opaque upon cooling, indicating the separation of water ice. Since Φ_s is the smallest in those samples that were observed to contain a crystalline ice phase, it is possible that Trp and RNase could have been occluded in the ice structure or otherwise associated with the crystallites, producing an environment characterized by rapid SLR. This possibility cannot be excluded by our measurements. Ice crystallization cannot be the only source of a population exhibiting rapid SLR, however. In the ice-free clear glass samples that form above 20% EG, Φ_s varies with composition (Figure 8) and does not exceed 0.7 in the range spanned by the clear glass samples (30−90% EG). Thus, distinct solvent environments that are characterized by either rapid or slow SLR are present in the aqueous EG glass in the absence of ice formation.

Although regions of heterogeneous composition probably are present to some extent in a solute-free aqueous glass containing a cryosolvent such as EG, we think it more likely that the present results arise from the organization of local solvent composition and/or structure by the solute molecules themselves. A large number of local solvent structures are likely to be present in dynamic equilibrium at ambient temperatures; some energetically more favorable of these would be frozen into the glass as the temperature is reduced. The distribution falls into two major classes, distinguished by large differences in the efficiency of SLR on the time scale determined by the triplet state decay.

The influence of solute on local solvent composition has been observed in some recent electrochemical studies. The effect of solvent composition in EG−water mixtures on the formal potentials of the ethylenediamine-*N*,*N*,*N*′,*N*′-tetraacetatovanadate(III/II) redox reaction have been interpreted[18] on the basis of differential solvation of the reactant and product. The more highly charged V(II) species is found to have much higher affinity for water in the solvation shell than does the V(III) species. The free energy of solvent reorganization associated with EG/H_2O interchange in the solvation shell that accompanies the redox reaction leads to readily observable and thermodynamically interpretable solvent-dependent shifts in the formal potential. It is possible that analogous organized local solvent shell structures are frozen out in our samples that manifest widely differing SLR behavior.

Currently, we are investigating possible sources of heterogeneous SLR in rigid solvents. Under study are the effects of solvent deuteration, polarity of the glass, changing the chromophore, the amino acid side chain, dissolved oxygen, glass vs crystalline solvent, and other possible factors that might influence SLR.

The work presented here makes clear the major reason previous experiments using the microwave-saturated phosphorescence decay method[8,19] to obtain the k_i and W_{ij} of Trp in EG−water solvent mixtures have led to erroneous results. The method relies on the assumption that the phosphorescence originates from a kinetically homogeneous triplet population. Thus far, this condition appears to be unachievable in EG−water solvent systems.

Acknowledgment. This publication was made possible by Grant ES-02662 from the National Institute of Environmental Health Sciences, NIH.

References and Notes

(1) Galley, W. C. In *Concepts of Biochemical Fluorescence*; Chen, R. F., Edelhoch, H., Eds.; Marcel Dekker: New York, 1976; Chapter 8.
(2) Hershberger, M. V.; Maki, A. H.; Galley, W. C. *Biochemistry* **1980**, *19*, 2204.
(3) Kwiram, A. L. In *Triplet State ODMR Spectroscopy;* Clarke, R. H., Ed.; Wiley: New York, 1982; p 427.
(4) Maki, A. H. In *Biological Magnetic Resonance;* Berliner, L. H., Reuben, J., Eds.; Plenum: New York, 1984; Vol. 6, p 187.
(5) Maki, A. H. *Methods Enzymol.* **1995**, *246*, 610.
(6) Ghosh, S.; Petrin, M.; Maki, A. H. *Biophys. J.* **1986**, *49*, 753.
(7) Brenner, H, C.; Kolubayev, V. *J. Lumin.* **1988**, *39*, 251.
(8) Zuclich, J.; von Schütz, J. U.; Maki, A. H. *Mol. Phys.* **1974**, *28*, 33.
(9) Ozarowski, A.; Wu, J. Q.; Maki, A. H. *J. Magn. Reson. A* **1996**, *121*, 178.
(10) Schmidt, J.; Veeman, W. S.; van der Waals, J. H. *Chem. Phys. Lett.* **1969**, *4*, 341.
(11) Wu, J. Q.; Ozarowski, A.; Maki, A. H. *J. Magn. Reson. A* **1996**, *119*, 82.
(12) Press: W. H.; Flannery, S. A.; Teukolsky, S. A.; Vetterling, W. T. *Numerical Recipes in Pascal;* Cambridge University Press: Cambridge, UK, 1989; p 326.
(13) Shain, A. L.; Sharnoff, M. *J. Chem. Phys.* **1973**, *59*, 2335.
(14) Kreyszig, E. *Advanced Engineering Mathematics*, 4th ed.; Wiley: New York, 1979; p 359.
(15) Wu, J. Q.; Ozarowski, A.; Davis, S. K.; Maki, A. H. *J. Phys. Chem.* **1996**, *100*, 11496.
(16) Ugurbil, K.; Maki, A. H.; Bersohn, R. *Biochemistry* **1977**, *16*, 901.
(17) Cordray, D. R.; Kaplan, L. R.; Woyciesjes, P. M.; Kozak, T. F. *Fluid Phase Equilib.* **1996**, *117*, *146.*
(18) Hecht, M.; Fawcett, W. R. *J. Phys. Chem.* **1996**, *100*, 14240.
(19) Rousslang, K. W.; Kwiram, A. L. *Chem. Phys. Lett.* **1976**, *39*, 231.